Systemic and local administration of lactoferrin promotes bone regeneration in non-critical-sized rat calvarial bone defects

Tomohiro Yoshimaki
Nihon University Graduate School of Dentistry,
Major in Periodontology
(Directors: Prof. Bunnai Ogiso and Assoc. Prof. Shuichi Sato)

Table of Contents

Abstract

Lactoferrin (LF) is an 80 kDa iron-binding glycoprotein that belongs to the transferrin family of proteins. LF increases the calcification of the extracellular matrix by osteoblasts, and inhibits differentiation of osteoclasts, suggesting a potential for LF in bone formation. Thus, the administration of LF may facilitate regeneration of bone loss in osteoporosis. The objective of this study was to evaluate the bone regenerative effect of LF in rat calvarial flat bone defects using *in vivo* micro computed tomography (micro-CT) and histological sections.

In the first chapter, the effect of systemic administration of LF on bone defect regeneration was examined in rat calvaria. Non-critical-sized calvarial bone defects sized approximately 2.7 mm in diameter were trephined into the dorsal part of the parietal bone on each side of the sagittal suture. An absorbable collagen sponge (ACS) soaked in saline was placed on each side. Rats devided into three experimental groups with 10 rats each were treated separately: control group (saline), 100-mg/kg group (100 mg LF/kg body weight), and 10-mg/kg group (10 mg LF/kg body weight). Intraperitoneal injection of LF or saline was carried out every day from day 0 to 4 weeks after the operation. Bone volume (BV) in 100-mg/kg group increased significantly in 1 to 4 weeks after the surgery. Histological analysis revealed a lager more number of osteoblast-like cells around the bony rim in 100-mg/kg group compared to the control group. Thus, systemic administration of LF promoted bone regeneration in non-critical-sized calvarial bone defects.

In the second chapter, the effect of local administration of LF on bone regeneration was examined in rat calvaria. Non-critical-sized calvarial bone defects (each 2.7 mm in diameter) were created as same procedure as the first chapter. ACS permeated with 5.5 mg LF was placed in the experimental LF side. ACS soaked in saline was placed in the control side. BV increased significantly after 3 and 4 weeks at LF sites compared to the control side. The mass of newly generated bone in LF side increased significantly at 4 weeks. Histological analysis revealed a larger number of osteoblast-like cells around the bony rim in LF side than in control side. Thus, local administration of LF promoted bone regeneration in non-critical-sized calvarial bone defects.

Conclusively, it was clearly demonstrated in this study that both systemic and local administration of LF promoted bone regeneration in non-critical-sized bone defects prepared experimentally in the rat calvarium. While the clinical application of LF could be possible via both systemic and local deliveries, the latter will be therapeutically more promising because the local application has definitely better controllability in terms of dose, range and frequency for the delivery of LF.

Chapter 1: Bone regeneration with systemic administration of lactoferrin in non-critical-sized rat calvarial bone defects

Tomohiro Yoshimaki, Shuichi Sato, Katsuyoshi Tsunori, Hiromichi Shino, Shinya Iguchi, Yoshinori Arai, Koichi Ito, Bunnai Ogiso

Introduction

Lactoferrin (LF) is an 80-kDa iron-binding glycoprotein in to the transferrin family of proteins (1). It is produced by many exocrine glands and is thus widely distributed in body fluids, including milk, saliva, tears, bile, and pancreatic fluid (2).

LF is a pleiotropic factor with a wide range of biological functions. As an iron-chelating agent, it may contribute to antibacterial action (3). It also affects cell growth and differentiation (4), embryonic growth (5), endothelial cell adhesion (6), cytokine production (7), immune system regulation (8), and inflammatory response modulation (9). An *in vitro* study showed that LF potently activates osteoblast proliferation and differentiation. In addition, alkaline phosphatase (ALP) activity also increased by LF (10).

Recent studies have shown that LF promotes bone growth (11, 12). Local injection of LF in the calvariae of adult mice for 5 consecutive days increased bone formation and bone area as compared with controls (11). In addition, oral administration of LF to ovariectomized (OVX) rats for 3 months protected from reduction caused in OVX of bone volume (BV) and mineral density (13). Bioresorbable collagen sponges loaded with growth factors, including bone morphogenic proteins (14), platelet-derived growth factor (15), and basic fibroblast growth factors (16), have been used to induce bone formation. In the present study, the effect of systemic administration of LF on bone defect regeneration were examined in rat calvaria.

Materials and Methods

Animals

Thirty 11-week-old male Fischer rats, weighing 250-300 g, were used. The animals were housed in an experimental animal room (22°C, 55% humidity, 12/12 h light/dark cycle) and fed a standard laboratory diet and water. The Animal Experimentation Committee of the Nihon University School of Dentistry approved the present study (AP10D032-2).

Surgical procedure

After establishing general anesthesia with intraperitoneal (IP) sodium pentobarbital (30 mg/kg, Somnopentyl; Schering-Plough, Munich, Germany), the surgical area was shaved, the

skin was washed with 70% ethanol, and 0.5 ml 2% lidocaine (Xylocaine; Astra-Zeneca, Osaka, Japan) was injected into the periosteum to control bleeding and provide additional local anesthesia.

A horseshoe-shaped skin incision was made over the head, the parietal area was exposed under aseptic conditions, and the periosteum was elevated to expose the bone. Non-critical-sized calvarial bone defects (diameter 2.7 mm) were trephined into the dorsal bone on both side of the midsagittal suture (Fig. 1a). Defects were created using a dental surgical drilling unit with a trephine, which was cooled constantly with sterile saline. Then, the calvarial disk was carefully removed to avoid tearing the dura. After thoroughly rinsing the area with physiological saline solution to wash out any bone fragments, An absorbable collagen sponge (ACS) (Teruplug®; Terumo Co., Tokyo, Japan) was placed (Fig. 1b). The skin incision was closed with 4-0 silk sutures (Ethicon Inc., Somerville, NJ, USA). The day of surgery was designated as day 0.

LF Administration

Rats were randomly assigned to three groups of 10 rats each and given the following treatments of bovine LF (Wako Pure Chemical Industries, Osaka, Japan): 100 mg/kg, 10 mg/kg solution of LF or saline (100-mg/kg, 10-mg/kg groups and control group, respectively). IP injection of LF or saline was done every day from day 0 to 4 weeks after the operation.

Imaging system

The *in vivo* micro computed tomography (micro-CT)(R_mCT; Rigaku Co., Tokyo, Japan) has a microfocus X-ray tube with a focal point of 7 μm, and an X-ray sensor with a 4-inch image intensifier. The X-ray source and image intensifier are connected by a basal plate, and the I-arm rotates on the vertical plane and is driven by a direct-drive motor. Rats were anesthetized with sodium pentobarbital and placed on the stage, and images of the areas of interest were captured. Repeated micro-CT imaging was performed from 1 to 4 weeks after surgery.

Micro-CT

The exposure parameters were 90 kV and 88 μA. The images were reconstructed on a personal computer using the I-View software (I-View Image Center, Tokyo, Japan). Using BV-measuring software (Kitasenjyu Radist Dental Clinic, I-View Image Center), voxel images were used to measure BV within the cylinder; gray values and numbers of voxels with corresponding gray values were calculated in regions of interest (ROIs; Fig. 2). Bone mineral density (BMD) phantoms of 200, 300, 400, 500, 600, 700, and 800 mg hydroxyapatite/cm^3 with epoxy resin (Ratoc Engineering Co., Ltd., Tokyo, Japan) were scanned with the

micro-CT under the same conditions used for the rats in this study. BMD was calculated using X-ray absorption values obtained from raw micro-CT data. The X-ray absorption threshold was determined to be 400 mg/cm^3. ROIs were defined on the bone defects, each of which had a diameter of 2.7 mm and a height of 3 mm. The amount of new bone growth in each ROI was then determined. BV was calculated by multiplying the number of pixels with > 400 mg/cm^3 BMD by the volume of one pixel. BV in the ROIs was measured on day 0 and each week thereafter under the same conditions. Increase in BV, which considered to indicate defect reossification, was then calculated by subtracting the BV on day 0 from each subsequent value. In this manner, the defect reossification ratio was calculated every week.

Correlations with BMD were calculated using the pixel values of X-ray absorption from BMD phantoms of 200, 300, 400, 500, 600, 700 and 800 mg hydroxyapatite/cm^3.

Histological analysis

Four weeks after surgery, the animals were sacrificed by deep anesthesia using sodium pentobarbital (100 mg/kg IP; Somnopentyl). The skin was dissected, and the defect sites were removed, along with the surrounding bone and soft tissues. Next, the specimens were fixed in 10% formalin, after which they were decalcified with a formic acid-sodium citrate decalcification solution for 1 week and embedded in paraffin wax. Then, coronal sections (thickness, 5 μm) through the center of each circular defect were prepared and processed for hematoxylin and eosin staining. Histological examination was performed under a light microscope equipped with a morphometric system (manufacturer's information) which was connected to a personal computer.

Defect closure was determined by measuring the distance between the defect margins, and was expressed as a percentage of the width of the total defect (Fig. 3). New bone area was measured by counting the number of pixels representing all tissues within the boundaries of the newly formed bone. The mean numbers of osteoblast-like cells in all new bone areas were determined manually under a light microscope at ×200 magnification (Fig. 3).

Serum collection

Blood was collected from the tail vein 4 weeks after the operation. The blood was centrifuged and serum was collected. Serum specimens were stored at -80°C. Calcium^{2+} (Ca^{2+}) and ALP concentrations were measured.

Statistical analysis

Means and standard deviations of reossification ratios were calculated each week. The Mann-Whitney U-test was used to compare mean reossification ratios between groups. The significance level for statistical analysis was set at $P < 0.05$. Statistical analyses were

4

performed using the SPSS software (ver. 16.0J for Windows; SPSS Inc., Chicago, IL, USA).

Results

Micro-CT

Newly generated bone was observed as early as 2 weeks after surgery in the LF groups. Reossification developed by extensions of growth from the bony rims at the lateral sides of the bone defects. Minimal new bone was observed in the control group (Figs. 4-6).

As compared with the control group, BV was significantly greater in the 100-mg/kg group at 1 week and later, and in the 10-mg/kg group at 2 weeks (Fig. 7).

Histological analysis

In the 100-mg/kg and 10-mg/kg groups, newly bone formed from the margins towards the centers of bone defects. Osteoblast-like cells were observed around the bony rims of 100-mg/kg and 10-mg/kg groups. The ACS structure was absorbed, and fibrous tissue, including osteoblasts and new bone, partially covered the LF sites (Figs. 8, 9). The control was filled with dense fibrous connective tissue; new bone formation near the defect rims was minimal (Fig. 10).

Histomorphometric analysis

Defect closure differed significantly between the 100-mg/kg group and control group (68.4% vs. 17.0%, respectively; $P < 0.05$). The 100-mg/kg group had significantly larger areas of new bone compared with control sites ($P < 0.05$; Table 1). There were more osteoblast-like cells in the 100-mg/kg and 10-mg/kg groups than in the control group ($P < 0.05$; Table 2).

Serum collection

There was no significant difference in serum Ca^{2+} concentration (Fig. 11). ALP increased with LF doses, but the differences between groups were not statistically significant (Fig. 12).

Discussion

Continuous administration of LF for 5 consecutive days tended to dose-dependently increase new bone formation in the calvariae of adult mice. In a previous study, a 4 mg dose induced changes that were 4-fold those observed in control animals. In the present study, it is shown that systemic administration of LF enhanced bone regeneration in non-critical-sized rat bone defects. LF concentration was determined which inhibited the bone resorption in OVX rat (13). This is the first report that systemic administration of LF promotes bone regeneration in bone defects.

Dietary administration of LF improved BMD in an OVX rat model (13, 17), which suggests that LF-induced improvement in bone metabolism is due to a direct local effect of LF on bone. However, it is uncertain whether dietary LF reaches systemic circulation. Therefore, LF was applied IP injection. Guo et al. (13) reported that serum Ca^{2+} concentration was inversely associated with LF dose and believed this explained the decrease in osteoporosis in OVX rats. In this study non-OVX rats, systemic LF administration did not affect serum Ca^{2+} level. Hou et al. (17) reported that serum ALP level increased in relation to LF dose. The present study showed that serum ALP levels tended to increase depending on the LF dose; however, the difference was not statistically significant.

As compared with the control, production of osteoblast-like cells at wound sites was more than doubled in rats given LF. A previous study using primary rat osteoblasts cultured for 3 weeks found that bone nodule formation (a process that involves bone matrix deposition and mineralization by differentiated osteoblasts) depended on LF dosage and that both the range of mineralized bone formation and number of nodules increased. LF was strongly related to proliferation of primary osteoblast cells and osteoblastic cell lines and increased osteoblast differentiation (18). The mitogen stimulatory action of LF on osteoblast cells is mainly mediated by low-density lipoprotein receptor-related protein 1 (19).

According to Cornish et al. (11), LF has an anabolic action of osteoblast and inhibitory action of osteoclast cells *in vitro*, which suggest that it positively affects BV *in vivo*. The present study showed that systemic administration of LF enhanced bone regeneration in non-critical-sized rat bone defects.

Mountziaris et al. (20) reported that control to inflammatory reaction promoted bone regeneration. Since inflammation is associated with a primary reduction in BV, an anti-inflammatory effect is useful for bone regeneration. It has been reported that LF has anti-inflammatory effect. Moreover, LF has a known clinical safety profile and is not carcinogenic or toxic (21, 22).

Several studies have shown that growth factors promote bone regeneration *in vivo* (12, 14-16). It can be considered that the advantages of LF over other growth factors include its cost effectiveness (12) and safety. In addition, LF can be administered in bovine milk, along with other dietary elements or supplements. Thus, it is also more practical than other growth factors.

Chapter 2: Bone regeneration with local administration of lactoferrin in non-critical-sized rat calvarial bone defects

Tomohiro Yoshimaki, Shuichi Sato, Risa Kigami, Noriko Tsuchiya,
Shigeki Oka, Yoshinori Arai, Koichi Ito
Journal of Medical and Biological Engineering (in press)

Introduction

LF is a pleiotropic factor with a vast range of biological functions, and taken in the form of supplement. Recent studies have shown that LF promotes bone growth (11, 12). In addition, oral LF administration to OVX rats for 3 months protected against OVX induced reduction of BV and mineral density (13). In the chapter 1 reported that systemic administration of LF accelerated bone regeneration in non-critical-sized rat calvarial bone defects, as confirmed by micro-CT and histological analysis. Moreover, local injection of LF above the hemicalvariae of adult mice for 5 consecutive days increased bone formation and bone area compared with controls (11).

Bioresorbable collagen sponges loaded with growth factors, including bone morphogenic proteins (14), platelet-derived growth factor (15), and basic fibroblast growth factors (16), have been used to induce bone formation. ACS containing fibrillar atelocollagen has been developed to minimize antigenicity, with biocompatibility achieved through cross-linking by heat treatment (18). This material has an adequate residual volume, providing sufficient space for the maintenance of mechanical properties and surrounding cell infiltrate. Takayama et al. (23) suggested that collagen membrane could be used as an LF carrier in bone tissue engineering. However, the direct effects of LF on bone defects have received little attention *in vivo*. In the present study, the effect of local administration of LF on bone defect regeneration were examined in rat calvaria.

Materials and methods

Animals

Ten 11-week-old male Fischer rats weighing 250-300 g each were used. The animals housed same condition in the chapter 1. The Animal Experimentation Committee of the Nihon University School of Dentistry approved the present study (AP10D032-2).

Preparation of ACSs permeated with LF or saline solution

Circular pieces of ACS (3 mm diameter) containing 11 μl bovine LF solution (500 mg/ml, total 5.5 mg LF) were used as scaffolds. The permeated ACSs were air-dried at 4°C for 48 h

(Fig. 13), then applied to bone defects. ACSs permeated with 11 μl saline solution were applied to control sides.

Surgical procedure

Surgical procedure was carried out as described in chapter 1 (Fig. 14a). ACSs with or without LF were placed on the experimental and control sides (Fig. 14b). Skin closure was accomplished using 4-0 silk sutures (Ethicon). The day of surgery was designated as day 0.

Imaging system

Micro-CT system was used as described in chapter 1, repeated micro-CT imaging was performed from 1 to 4 weeks after surgery.

Micro-CT

Micro-CT analysis was used as described in chapter 1 (Fig. 2). In addition, correlations with BMD were calculated using the pixel values of X-ray absorption from BMD phantoms of 200, 300, 400, 500, 600, 700 and 800 mg hydroxyapatite/cm^3. BM was then calculated using the pixel values of X-ray absorption within ROIs in combination with BMD correlations.

Histological analysis

Histological analysis was carried out as described in chapter 1 (Fig. 3).

Statistical analysis

Means and standard deviations of reossification ratios were calculated every week. Mean reossification ratios in the two groups were compared using the Wilcoxon test. The significance level for statistical analysis was set at $P < 0.05$. Statistical analysis was performed using SPSS software (ver. 16.0J for Windows).

Results

Micro-CT

Newly generated bone was observed at LF sides as early as 2 weeks after surgery. The reossification developed by extensions of growth from the bony rims at the lateral sides of the bone defects. Minimal amounts of new bone were observed at control sides (Figs. 15, 16).

BV was significantly enhanced after 3 and 4 weeks at LF sides compared with control sides (1.70 *vs*. 1.13 mm^3 and 2.44 *vs*. 1.54 mm^3, respectively; $P < 0.05$; Fig. 17). BM at LF sides had increased significantly at 4 weeks (1.55 *vs*. 1.02 mg, respectively; $P < 0.05$; Fig. 18).

Histological analysis

At LF sides, newly generated bone formed from the margins toward the centers of the bone defects. Osteoblast-like cells were observed around the bony rims of LF sides. The ACS structure was absorbed, and fibrous tissue, including osteoblasts and new bone, partially covered LF sides (Fig. 19).

Control sides were filled with dense fibrous connective tissue, including minimal new bone formation near the defect rims (Fig. 20).

Histomorphometric analysis

Defect closure differed significantly between the LF and control sides (73.3% *vs*. 44.2%; *P* < 0.05). LF sides had significantly larger areas of new bone compared with control sides (12.7 *vs*. 6.6%; *P* < 0.05; Table 3). More osteoblast-like cells were observed at LF sides than at control sides (Table 4).

Discussion

In the chapter 1, it was revealed that systemic administration of LF enhanced bone regeneration in non-critical-sized rat bone defects. These findings suggest that LF-induced improvement in bone metabolism may be a result of LF's direct local effect on bone. Therefore, LF-permeated ACSs was applied directly to bone defects. This local application of LF effectively induced bone regeneration.

ACS was used as a carrier for LF. ACS consists of type I collagen and has been used widely in regenerative studies (14-16). Takayama et al. (23) described the profile of LF release from the collagen membrane, reporting that 27% of LF was released within 1 h after incubation, but only 30% of LF was released after 5 days. Thus, the rapid initial release of LF is followed by more gradual release from the collagen membrane. Takayama et al. (23) also demonstrated that human sarcoma-derived cells on an LF-permeated collagen membrane exhibited increased alkaline phosphatase activity and osteocalcin production. Thus, collagen membrane can be used as an LF carrier in bone tissue regeneration.

In culture with human osteosarcoma-derived cells, a collagen membrane permeated with 1 mg LF significantly promoted calcification compared with permeation with 0.5 mg LF. Sufficient LF (total, 5.5 mg) was applied to ACSs used to cover calvarial bone defects. Calcification may have been promoted by LF; i.e., a cell permeates and adheres to the ACS, and blood is contained within the calcification of the ACS. However, conditions of *in vitro* and *in vivo* studies have differed, and further studies are needed to determine the optimal LF dose for new bone regeneration.

The present study showed that local application of LF enhanced bone regeneration in non-critical-sized rat bone defects. Takaoka et al. (12) implanted gelatin hydrogels

incorporating 30 mg LF into 8-mm critical-sized bone defects in rat calvaria and observed bone regeneration. Their results showed significantly stronger bone regeneration at 8 weeks after surgery. In the present study, BV was significantly enhanced after 3 and 4 weeks at LF sides compared with control sides. The discrepancy in these results may be due to differences in bone defect size (2.7 mm *vs*. 8 mm), carrier type (collagen *vs*. hydrogel), or LF concentration.

BV and the number of osteoblast-like cells were tend to larger than chapter 1. Therefore, the local administration of LF may enhance the differentiation of osteoblast-like cells and osteoblast cell activity in bone defects.

In conclusion, local administration of LF is more effective in the bone regeneration compared to systemic administration of LF.

Conclusions

Within the limitation of the present study, the following conclusions were drawn:

1. Systemic administration of LF promoted bone regeneration in non-critical-sized bone defects in the rat calvarium.

2. Local administration of LF promoted bone regeneration in non-critical-sized bone defects in the rat calvarium.

Conclusively, it was clearly demonstrated in this study that both systemic and local administration of LF promoted bone regeneration in non-critical-sized bone defects prepared experimentally in the rat calvarium. While the clinical application of LF could be possible via both systemic and local deliveries, the latter will be therapeutically more promising because the local application has definitely better controllability in terms of dose, range and frequency for the delivery of LF.

References

1. Metz-Boutigue MH, Jollès J, Mazurier J, Schoentgen F, Legrand D, Spik G, Montreuil J, Jollès P (1984) Human lactoferrin: amino acid sequence and structural comparisons with other transferrins. Eur J Biochem 145, 659-676.

2. Lönnerdal B, Iyer S (1995) Lactoferrin: molecular structure and biological function. Annu Rev Nutr 15, 93-110.

3. Weinberg ED (2001) Human lactoferrin: a novel therapeutic with broad spectrum potential. J Pharm Pharmacol 53, 1303-1310.

4. Bi BY, Lefebvre AM, Duś D, Spik G, Mazurier J (1997) Effect of lactoferrin on proliferation and differentiation of the jurkat human lympoblastic T cell line. Arch Immunol Ther Exp 45, 315-332.

5. Ward PP, Mendoza-Meneses M, Mulac-Jericevic B, Cunningham GA, Saucedo-Cardenas O, Teng CT, Conneely OM (1999) Restricted spatiotemporal expression of lactoferrin during murine embryonic development. Endocrinology 140, 1852-1860.

6. Baveye S, Elass E, Fernig DG, Blanquart C, Mazurier J, Legrand D (2000) Human lactoferrin interacts with soluble CD14 and inhibits expression of endothelial adhesion molecules, E-selectin and ICAM-1, induced by the CD14-lipopolysaccharide complex. Infect Immun 68, 6519-6525.

7. Cornish J (2004) Lactoferrin promotes bone growth. Biometals 7, 331-335.

8. Frydecka I, Zimecki M, Bocko D, Kosmaczewska A, Teodorowska R, Ciszak L, Kruzel M, Wlodarska-Polinsk J, Kuliczkowski K, Kornafel J (2002) Lactoferrin-induced up-regulation of zeta (ζ) chain expression in peripheral blood T lymphocytes from cervical cancer patients. Anticancer Res 22, 1897-1901.

9. Baveye S, Elass E, Mazurier J, Spik G, Legrand D (1999) Lactoferrin: a multifunctional glycoprotein involved in the modulation of the inflammatory process. Clin Chem Lab Med 37, 281-286.

10. Yagi M, Suzuki N, Takayama T, Arisue M, Kodama T, Yoda Y, Otsuka K, Ito K (2009) Effects of lactoferrin on the differentiation of pluripotent mesenchymal cells. Cell Biol Int 33, 283-289.

11. Cornish J, Callon KE, Naot D, Palmano KP, Banovic T, Bava U, Watson M, Lin JM, Tong PC, Chen Q, Chan VA, Reid HE, Fazzalari N, Baker HM, Baker EN, Haggarty NW, Grey AB, Reid IR (2004) Lactoferrin is a potent regulator of bone cell activity and increases bone formation in vivo. Endocrinology 145, 4366-4374.

12. Takaoka R, Hikasa Y, Hayashi K, Tabata Y (2011) Bone regeneration by lactoferrin released from a gelatin hydrogel. J Biomater Sci-Polym Ed 22, 1581-1589.

13. Guo HY, Jiang L, Ibrahim SA, Zhang L, Zhang H, Zhang M, Ren FZ (2009) Orally administered lactoferrin preserves bone mass and microarchitecture in ovariectomized

rats. J Nutr 139, 958-964.

14. Hasegawa Y, Sato S, Takayama T, Murai M, Suzuki N, Ito K (2008) Short-term effects of rhBMP2 enhanced bone augmentation beyond the skeletal envelope within a titanium cap in rabbit calvarium. J Periodontol 79, 348-354.

15. Tsuchiya N, Sato S, Kigami R, Yoshimaki T, Arai Y, Ito K (2013) Effects of platelet-derived growth factor on enhanced bone augmentation beyond the skeletal envelope within a plastic cap in the rat calvarium. J Hard Tissue Biol 22, 221-226.

16. Kigami R, Sato S, Tsuchiya N, Yoshimaki T, Arai Y, Ito K (2013) FGF-2 angiogenesis in bone regeneration within critical-sized bone defects in rat calvaria. Implant Dent 22, 422-427.

17. Hou JM, Xue Y, Lin QM (2012) Bovine lactoferrin improves bone mass and microstructure in ovariectomized rats via OPG/RANKL/RANK pathway. Acta Pharmacol Sin 33, 1277-1284.

18. Koide M, Osaki K, Konishi J, Oyamada K, Katakura T, Takahashi A, Yoshizato K (1993) A new type of biomaterial for artificial skin: dehydrothermally cross-linked composites of fibrillar and denatured collagens. J Biomed Mater Res 27, 79-87.

19. Grey A, Banovic T, Zhu Q, Watson M, Callon K, Palmano K, Ross J, Naot D, Reid IR, Cornish J (2004) The low-density lipoprotein receptor-related protein 1 is mitogenic receptor for lactoferrin in osteoblastic cells. Mol Endocrinol 18, 2268-2278.

20. Mountziaris PM, Mikos AG (2008) Modulation of the inflammatory response for enhanced bone tissue regeneration. Tissue Eng 14, 179-186.

21. Kruger CL, Marano KM, Morita Y, Takada Y, Kawakami H, Kobayashi T, Sunaga M, Furukawa M, Kawamura K (2007) Safety evaluation of a milk basic protein fraction. Food Chem Toxicol 45, 1301-1307.

22. Tamano S, Sekine K, Takase M, Yamauchi K, Iigo M, Tsuda H (2008) Lack of chronic oral toxicity of chemo preventive bovine lactoferrin in F344/DuCrj Rats. Asian Pac J Cancer Prev 9, 313-316.

23. Takayama Y, Mizumachi K (2009) Effect of lactoferrin-embedded collagen membrane on ostogenic differentiation of human osteoblastic-like cells. J Biosci Bioeng 107, 191-195.

Table 1

Defect closure

100-mg/kg group	68.4 ± 29.2	
10-mg/kg group	31.6 ± 13.5	*
Control	17.0 ± 8.7	

(%: group means ± SD, n = 10)　　* Mann-Whitney U-test, $P < 0.05$

Newly generated bone area

100-mg/kg group	53.2 ± 22.9	
10-mg/kg group	25.5 ± 15.6	*
Control	17.9 ± 5.9	

(%: group means ± SD, n = 10)　　* Mann-Whitney U-test, $P < 0.05$

Table 2

The number of osteoblast-like cells

100-mg/kg group	333.6 ± 62.3	
10-mg/kg group	201.8 ± 26.5	*
Control	121.4 ± 44.8	*

(cells: group means ± SD, n = 10)　　* Mann-Whitney U-test, $P < 0.05$

Table 3

Defect closure

LF	73.3 ± 19.1	**
Control	44.2 ± 26.8	

(%: group means ± SD, n = 10)　　** Wilcoxon test, $P < 0.05$

Newly generated bone area

LF	12.7 ± 5.5	**
Control	6.6 ± 4.2	

(%: group means ± SD, n = 10)　　** Wilcoxon test, $P < 0.05$

Table 4

The number of osteoblast-like cells

LF	382.7 ± 162.7	**
Control	165.5 ± 64.1	

(cells: group means ± SD, n = 10)　　** Wilcoxon test, $P < 0.05$
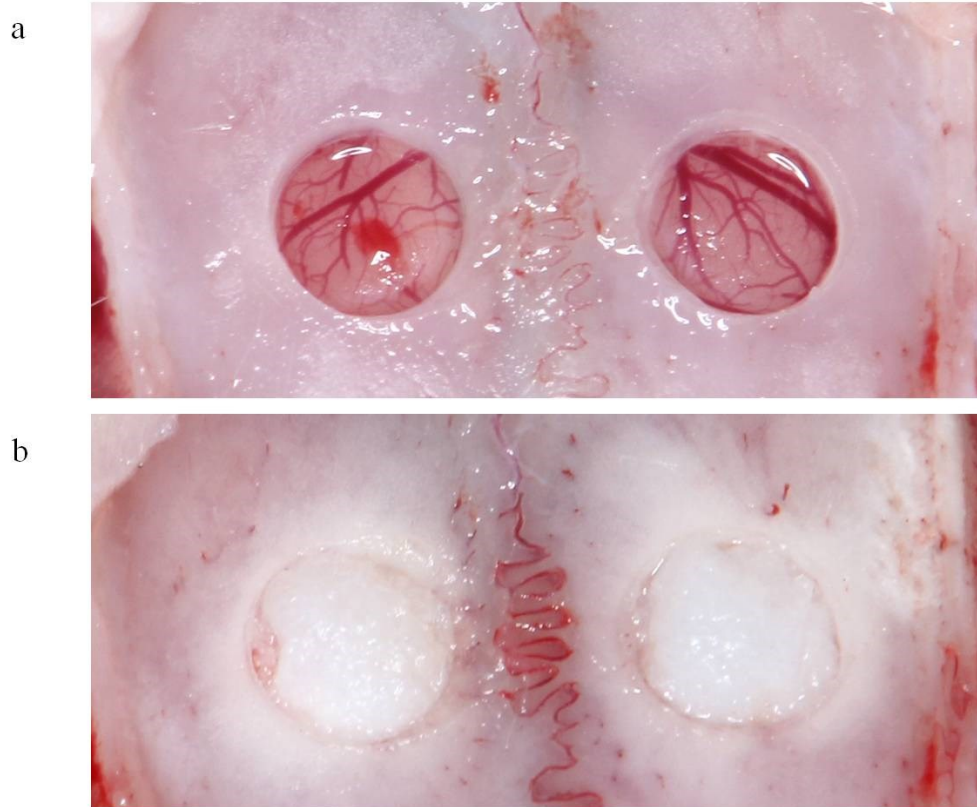
Fig 1. (a) Non-critical-sized calvarial bone defects (each 2.7 mm in diameter). (b) ACS soaked in saline was placed.
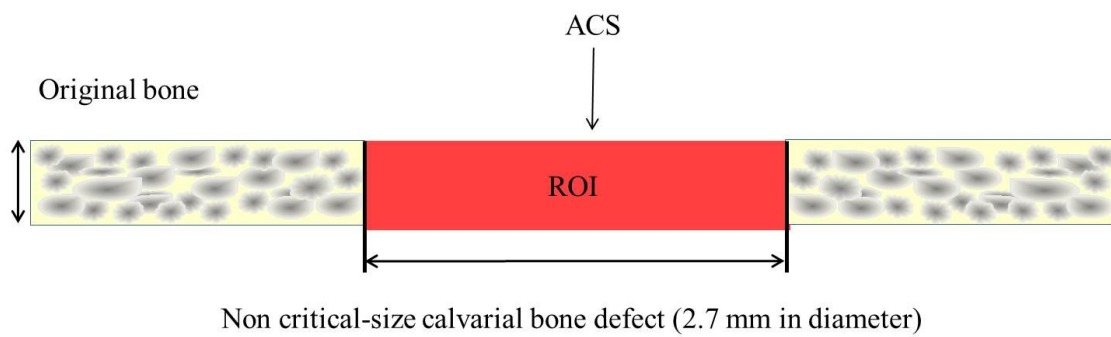
Fig 2. Observation area visualized by micro-CT.

a

b

Original bone

Newly generated bone area

Defect closure (%) (a-b)/a × 100
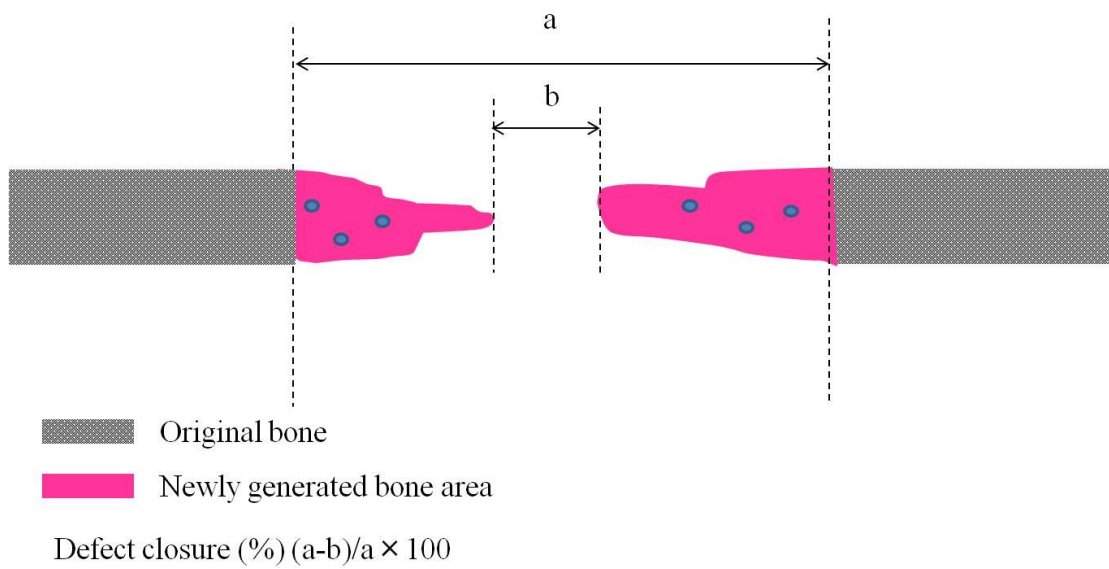
Fig 3. Schematic drawing of osteotomy calvarial defects, showing histometric analysis.

	0 w	1 w	2 w	3 w	4 w
X					
Y					
Z					
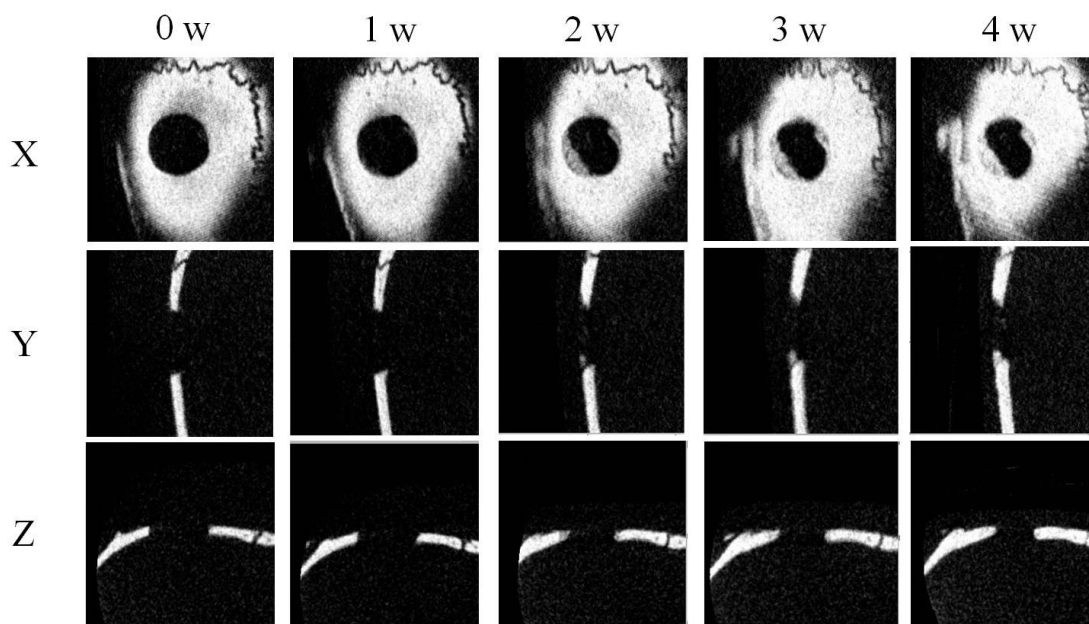
Fig 4. *x-y-z* image of 100-mg/kg group.
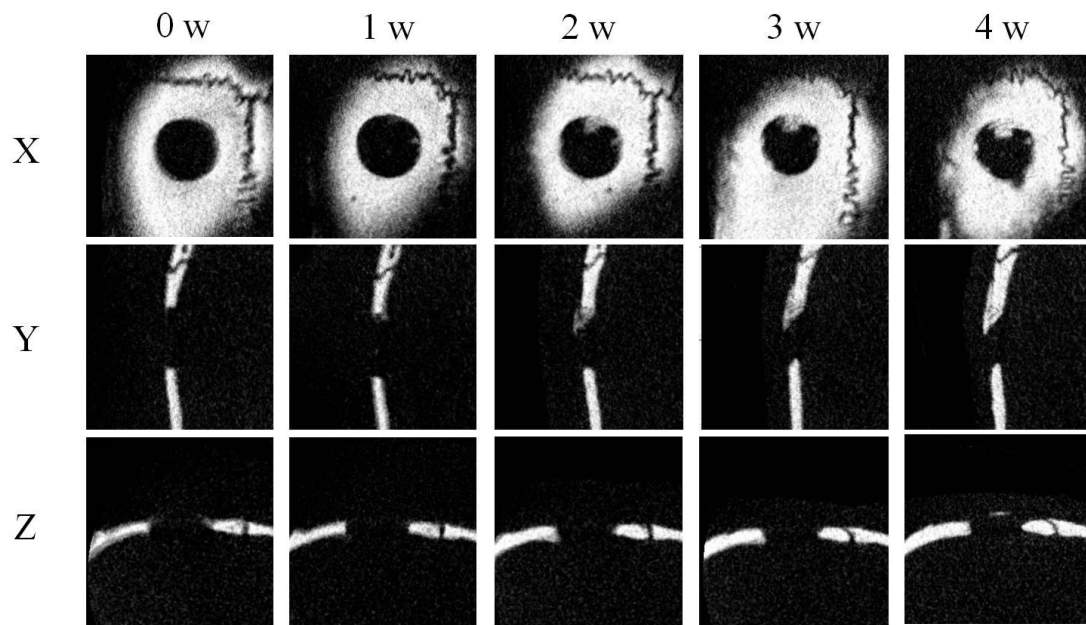
Fig 5. *x-y-z* image of 10-mg/kg group.
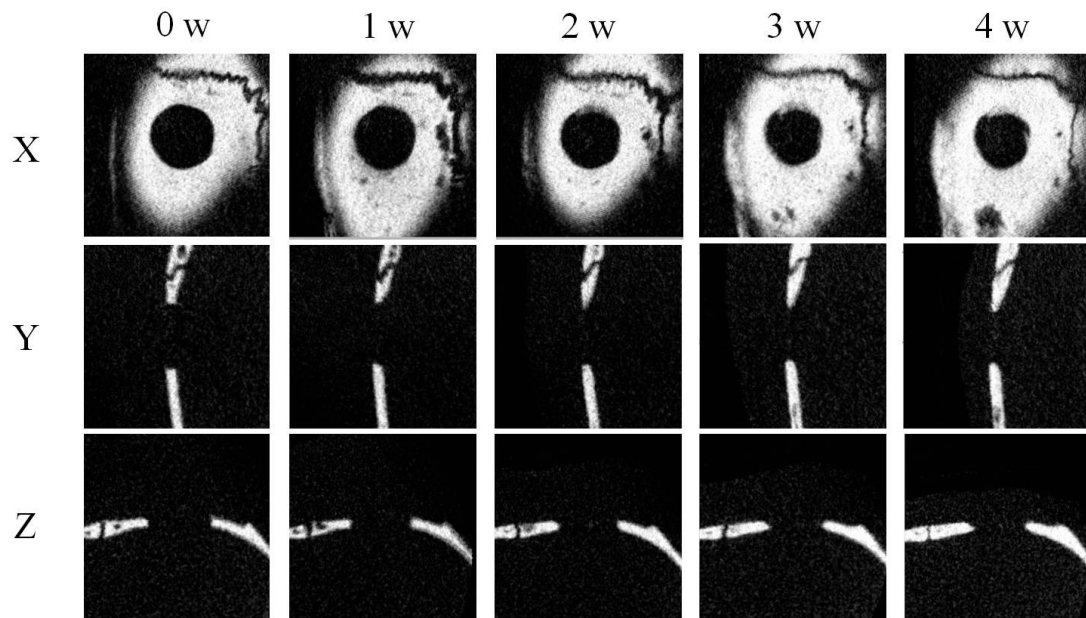
Fig 6. *x-y-z* image of control group.
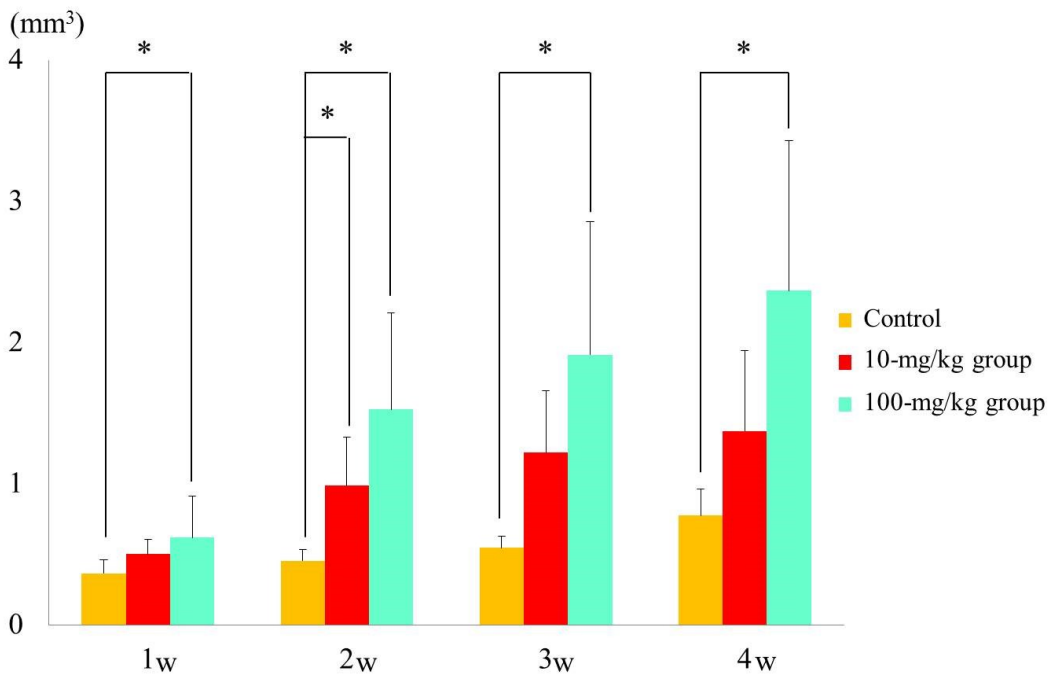
* Mann-Whitney U-test, *P* < 0.05

Fig 7. Volume of newly generated bone.

NB: newly generated bone
Ob: osteoblast-like cells
C: connective tissue
EB: existing bone
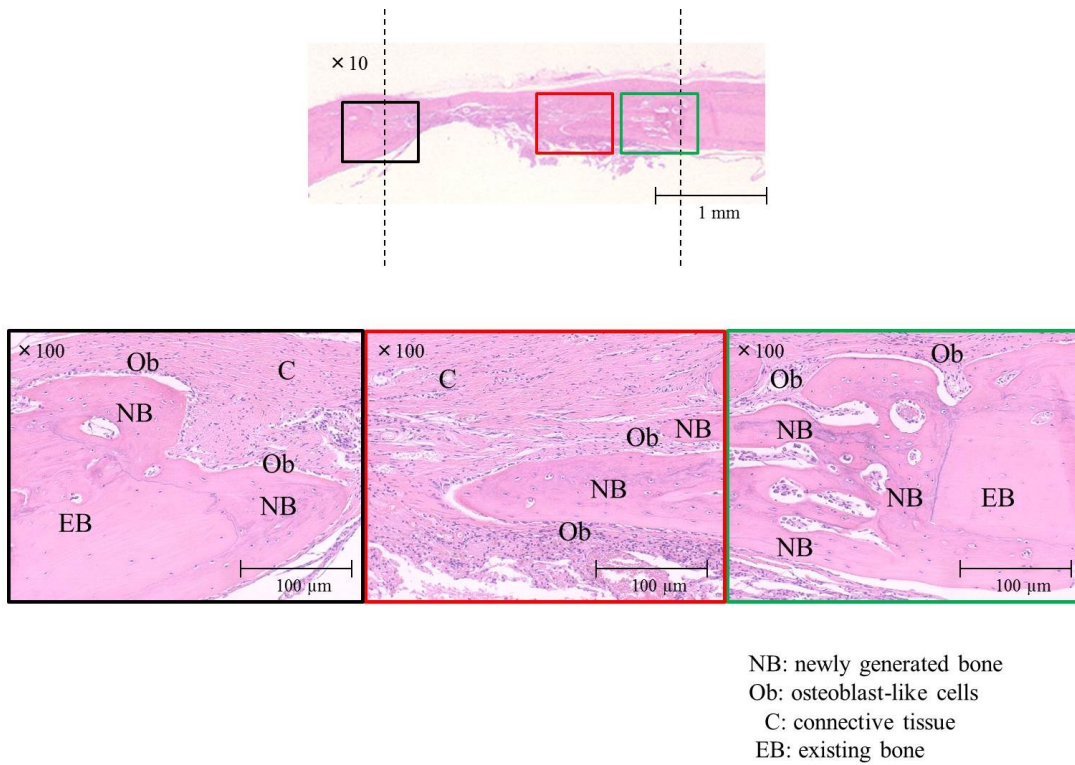
Fig 8. Representative histological sections from the 100-mg/kg group at 4 weeks after surgery.

NB: newly generated bone
Ob: osteoblast-like cells
C: connective tissue
EB: existing bone
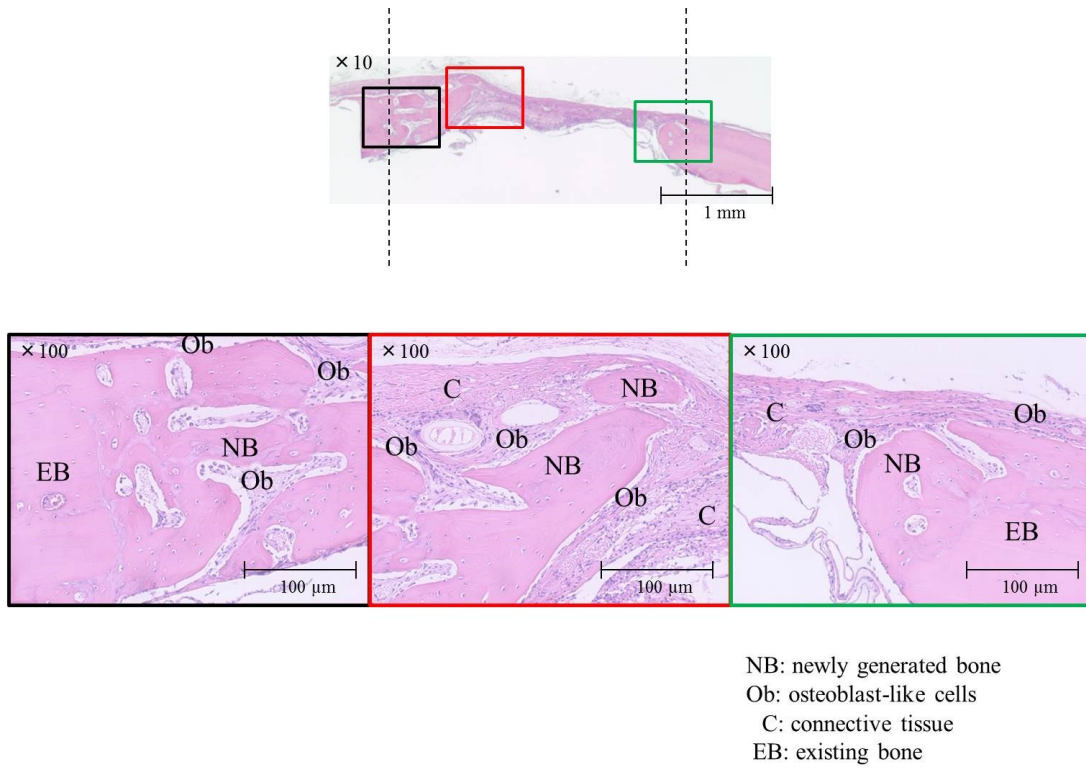
Fig 9. Representative histological sections from the 10-mg/kg group at 4 weeks after surgery.

NB: newly generated bone
Ob: osteoblast-like cells
C: connective tissue
EB: existing bone
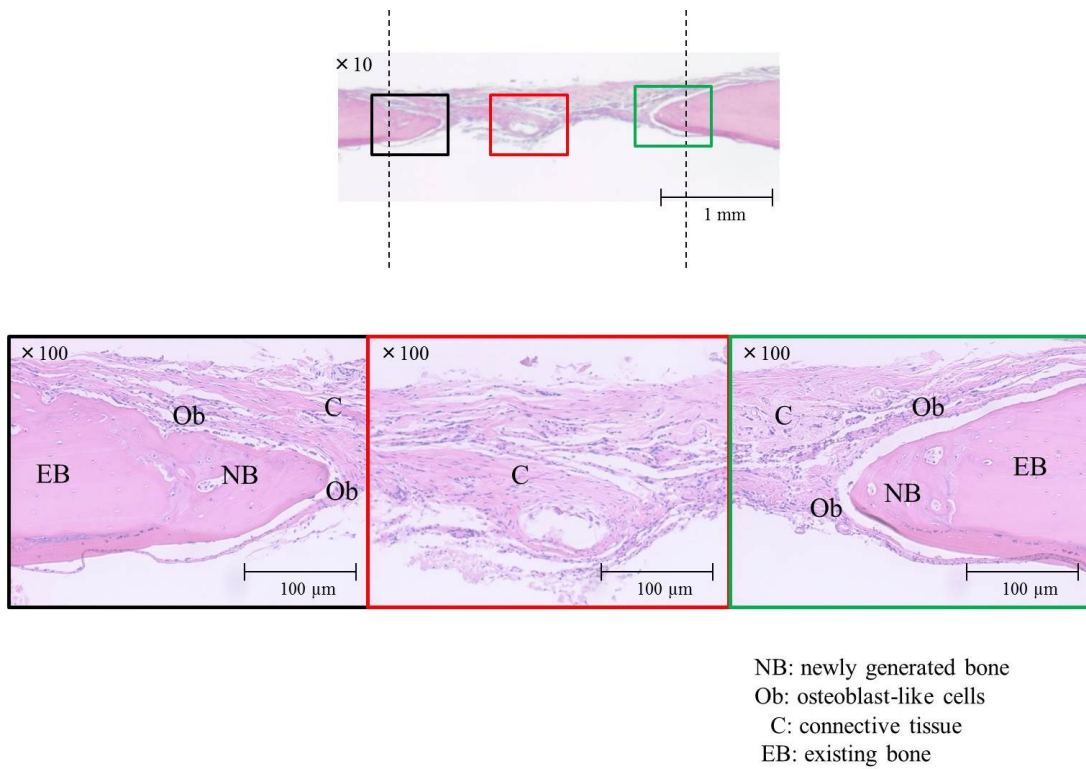
Fig 10. Representative histological sections from the control group at 4 weeks after surgery.
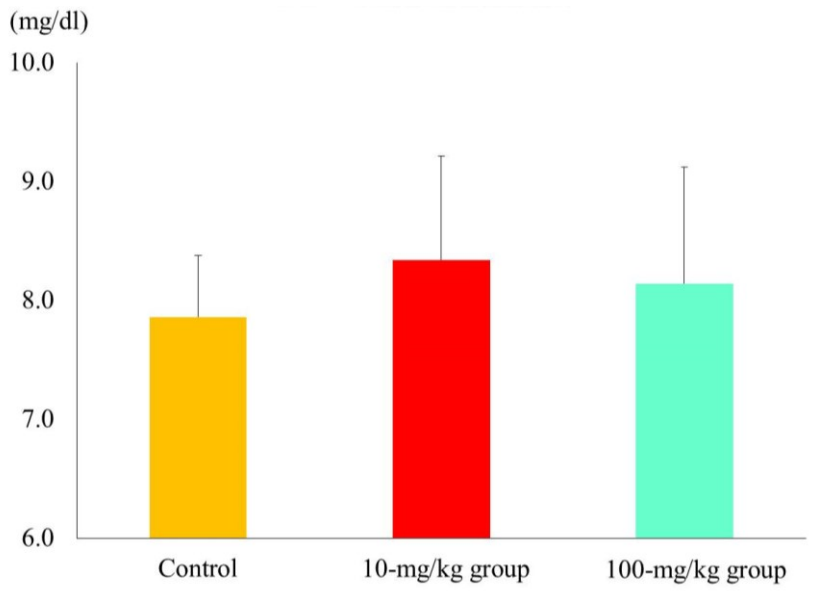
Fig 11. Ca^{2+} concentration in serum.
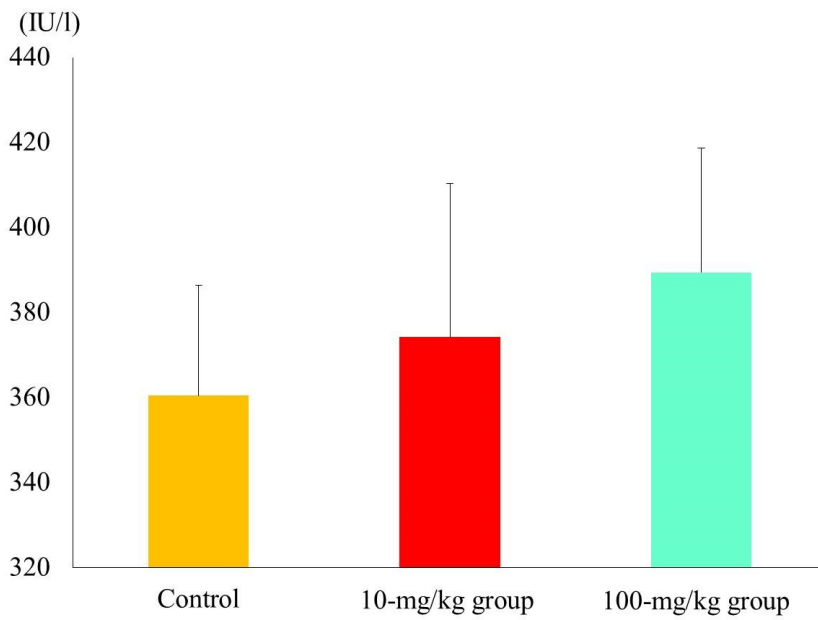
Fig 12. ALP concentration in serum.
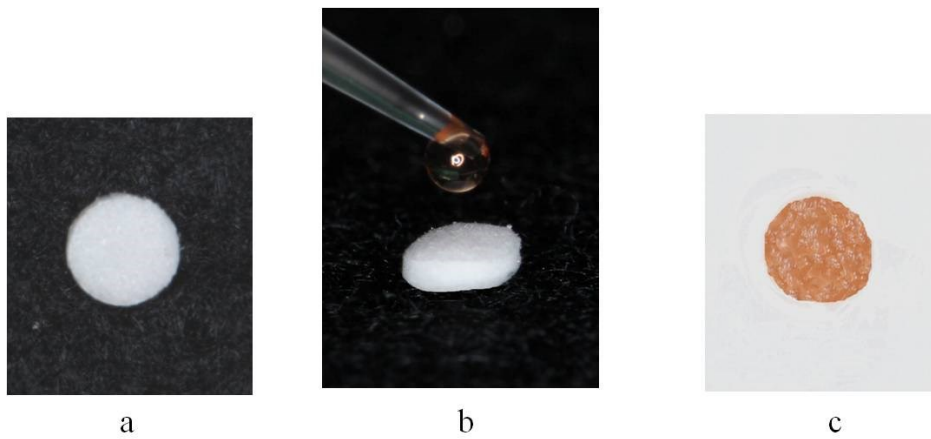
Fig 13. (a) ACS was cut into 3 mm disks. (b) The ACS was permeated with 11 μl LF solution at a concentration of 500 mg/ml. (c) The ACS was air-dried at 4°C for 48 h.
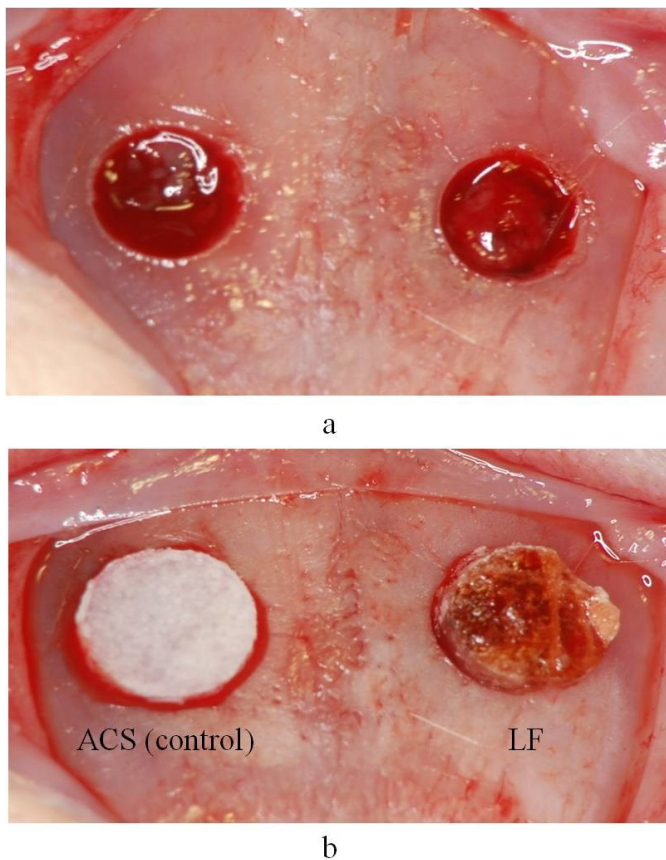
Fig 14. (a) Non-critical-sized calvarial bone defects (each 2.7 mm in diameter). (b) ACS permeated with LF solution (500 mg/ml, total 5.5 mg) was placed at the LF side, and a saline-permeated ACS was placed at the control side.
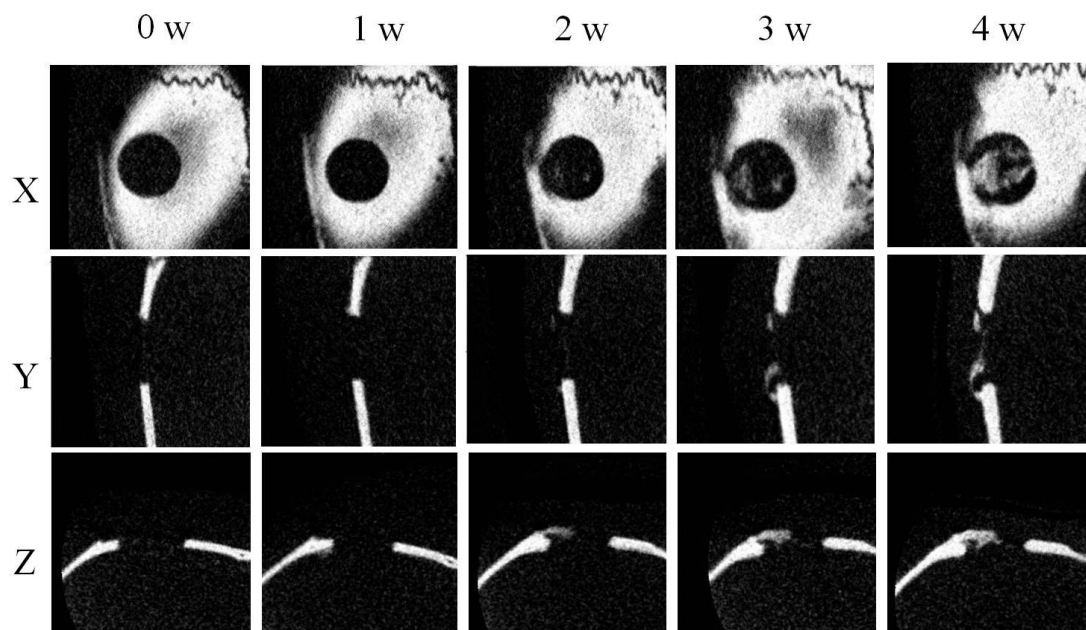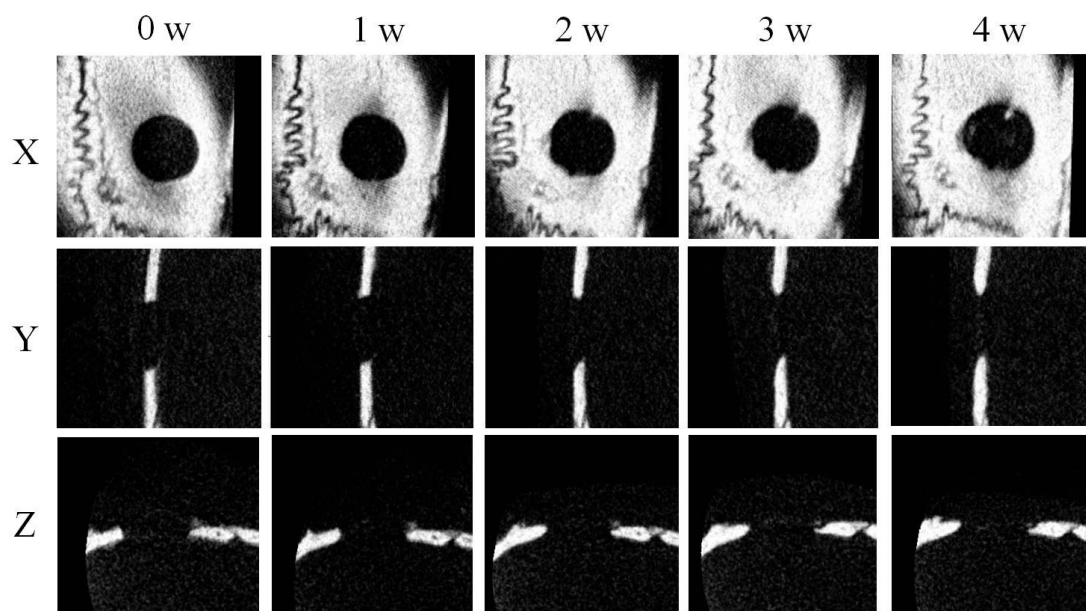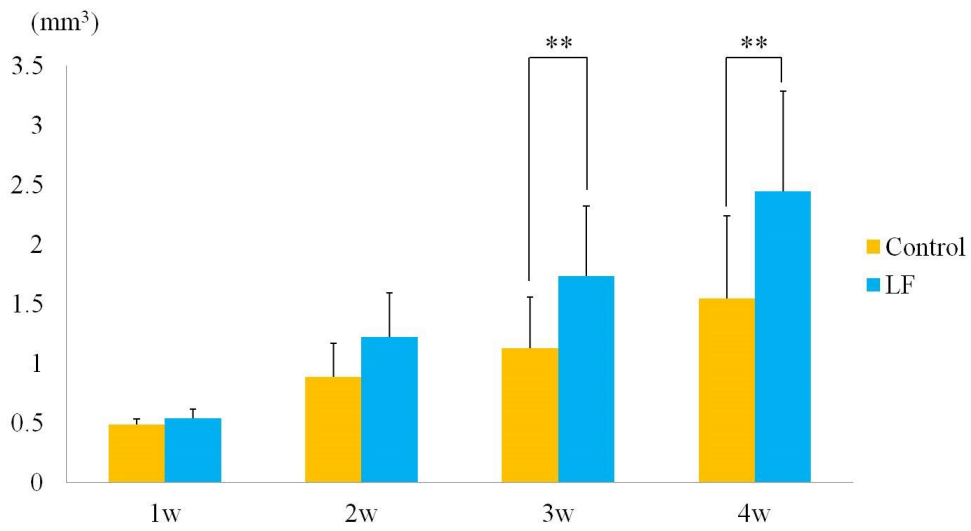
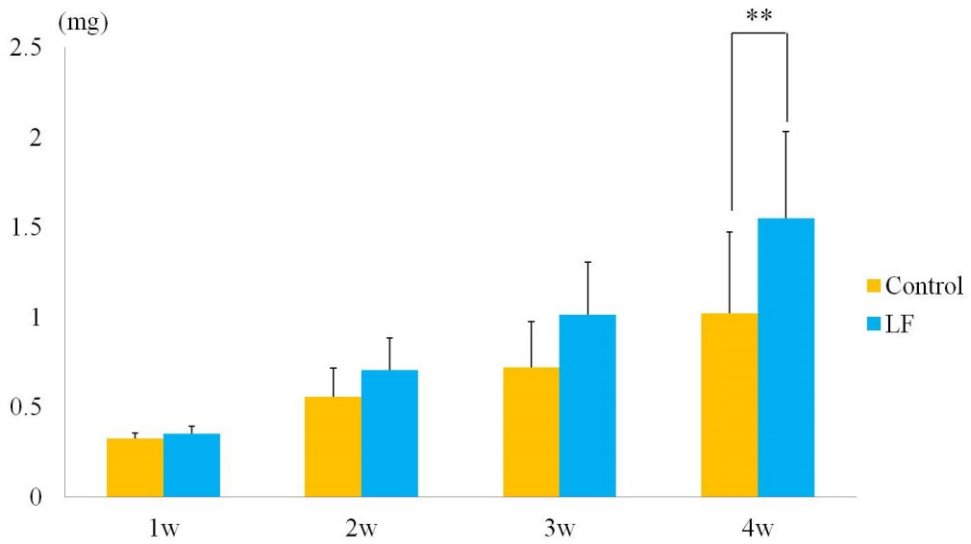Fig 15. *x-y-z* image of LF treated side.

Fig 16. *x-y-z* image of the control side.

**Wilcoxon test, *P* < 0.05

Fig 17. Volume of newly generated bone.

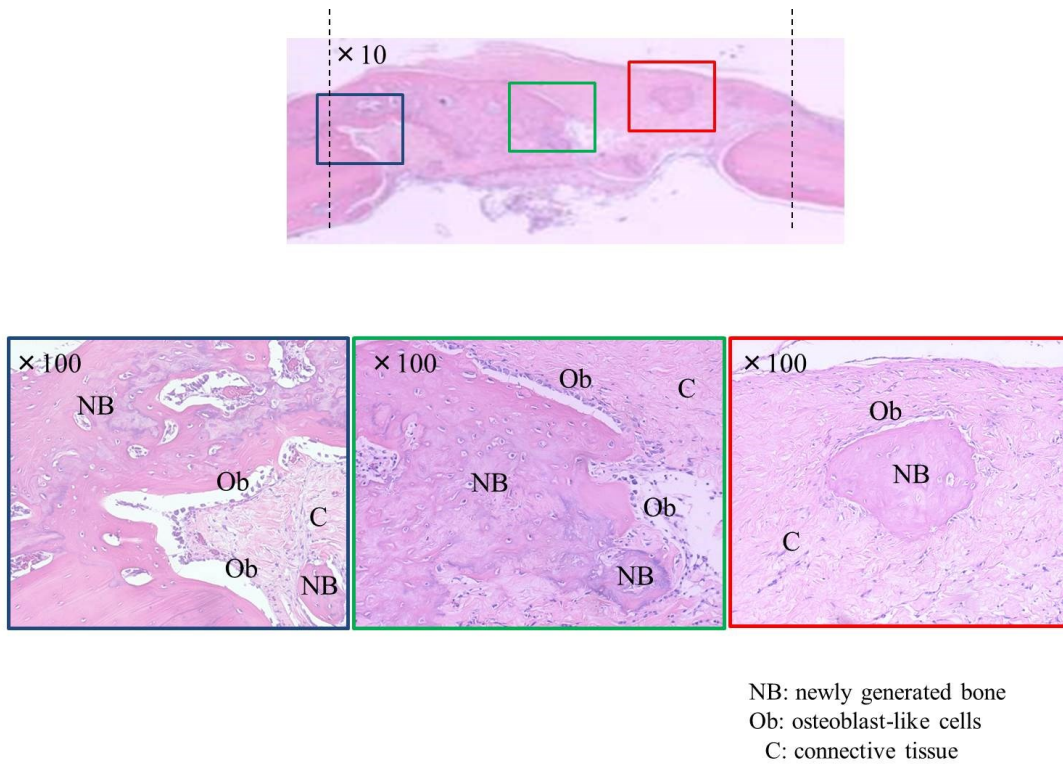**Wilcoxon test, *P* < 0.05

Fig 18. Mass of newly generated bone.

NB: newly generated bone
Ob: osteoblast-like cells
C: connective tissue

Fig 19. Representative histological sections of LF side at 4 weeks after surgery.

NB: newly generated bone
Ob: osteoblast-like cells
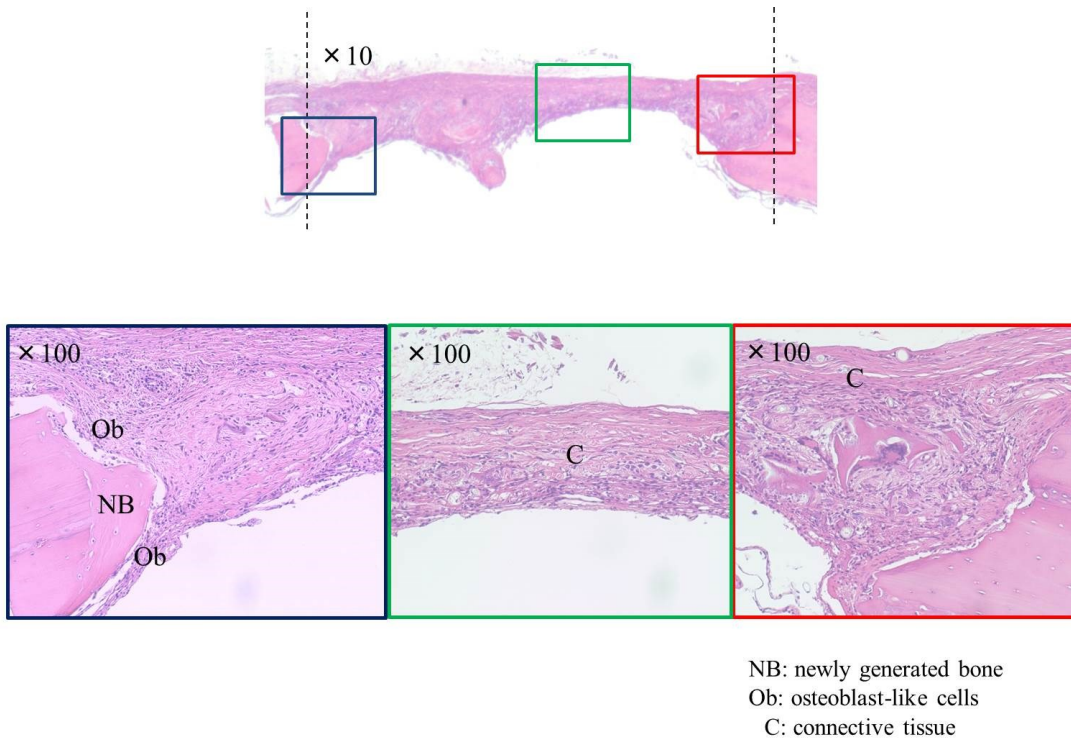C: connective tissue

Fig 20. Representative histological sections of control side at 4 weeks after surgery.